

# Exclusive Double Charmonium Production from $\Upsilon$ Decay

Yu Jia\*

*Institute of High Energy Physics, Chinese Academy of Sciences, Beijing 100049, China*

(Dated: February 1, 2008)

## Abstract

The exclusive decay of  $\Upsilon$  to a vector plus pseudoscalar charmonium is studied in perturbative QCD. The corresponding branching ratios are predicted to be of order  $10^{-6}$  for first three  $\Upsilon$  resonances, and we expect these decay modes should be discovered in the prospective high-luminosity  $e^+e^-$  facilities such as super  $B$  experiment. As a manifestation of the short-distance loop contribution, the relative phases among strong, electromagnetic and radiative decay amplitudes can be deduced. It is particularly interesting to find that the relative phase between strong and electromagnetic amplitudes is nearly orthogonal. The resonance-continuum interference effect for double charmonium production near various  $\Upsilon$  resonances in  $e^+e^-$  annihilation is addressed.

arXiv:0706.3685v1 [hep-ph] 25 Jun 2007

---

\* Electronic address: jia@ihep.ac.cn

## I. INTRODUCTION

Very rich  $J/\psi$  decay phenomena have historically served as an invaluable laboratory to enrich our understanding toward the interplay between perturbative and nonperturbative QCD [1, 2]. By contrast, much fewer decay channels of  $\Upsilon$  are known to date. It would be definitely desirable if more knowledge about bottomonium decay can be gleaned.

The typical branching fraction for a given hadronic decay mode of  $\Upsilon$  is in general much smaller than that of  $J/\psi$ . It is partly due to the smaller QCD coupling at the  $b$  mass scale than at the  $c$  scale, and more importantly, it is because the branching ratio gets diluted by a scaling factor of  $(m_c/m_b)^n$  when descending from charmonium to bottomonium (here  $n$  is some number no less than 4). These might intuitively explain why very few exclusive decay modes of bottomonia have been seen so far.

Due to rather large  $b$  mass,  $\Upsilon$  not only can dematerialize into light hadrons, it also can decay to charmful final states. In this work, we plan to study the exclusive decay of  $\Upsilon$  into double charmonium, or more specifically,  $J/\psi(\psi')$  plus  $\eta_c(\eta'_c)$ . The hard scales set by  $b$  and  $c$  masses in this type of processes justify the use of perturbative QCD (pQCD). Since the involved mesons are all heavy quarkonium, it is natural to employ NRQCD factorization approach [3]. This work constitutes a continuation of previous studies on bottomonium decay to double charmonium, namely,  $\chi_b, \eta_b \rightarrow J/\psi J/\psi$  [4, 5]. Although these decay modes have not yet been seen, some experimental information have already been available for inclusive  $J/\psi$  ( $\psi'$ ) production rate from  $\Upsilon$  decay [6, 7, 8]:

$$\begin{aligned}\mathcal{B}[\Upsilon(1S) \rightarrow J/\psi + X] &= (6.5 \pm 0.7) \times 10^{-4}, \\ \mathcal{B}[\Upsilon(1S) \rightarrow \psi' + X] &= (2.7 \pm 0.9) \times 10^{-4}, \\ \mathcal{B}[\Upsilon(2S) \rightarrow J/\psi + X] &< 6 \times 10^{-3}, \\ \mathcal{B}[\Upsilon(4S) \rightarrow J/\psi + X] &< 1.9 \times 10^{-4}.\end{aligned}\tag{1}$$

These inclusive decay ratios set upper bounds for our exclusive processes. It is worth noting that  $\Upsilon \rightarrow J/\psi \eta_c$  violates the hadron helicity conservation [9, 10]. It is thus natural to expect that the corresponding branching fractions are very suppressed.

One important impetus of this work is from the double charmonium production at  $\Upsilon(4S)$  resonance measured by Belle in 2002 [11]. The observed cross section is usually entirely ascribable to the continuum contribution because of rather broad  $\Upsilon(4S)$  width. Nevertheless for a full understanding, it is worth knowing precisely the impact of the resonant decay on the measured double charmonium cross section. Furthermore, stimulated by Belle's discovery, a natural question may arise—what is the discovery potential for double charmonium production in  $e^+e^-$  experiments operated at lower  $\Upsilon$  peaks? Since the first three  $\Upsilon$  resonances are much narrower than  $\Upsilon(4S)$ , the resonant decay contribution should dominate over the continuum one. Our study is motivated to answer this question.

One interesting problem in exclusive decays of a vector quarkonium is to know the relative phase between strong and electromagnetic amplitudes. For example, the corresponding relative phase in  $J/\psi \rightarrow PV$  ( $P, V$  stand for light  $0^{-+}$  and  $1^{--}$  mesons) has been extensively studied and found to be nearly orthogonal [12, 13, 14, 15, 16, 17]. In our case, the relative phase naturally emerges as a short-distance effect and thus is perturbatively calculable. Curiously, it is also found to be approximately orthogonal.

The rest of the paper is organized as follows. In Section II, we present the lowest-order NRQCD calculation for the decay process  $\Upsilon \rightarrow J/\psi + \eta_c$ , including strong, electromagnetic

and radiative decay channels. In Section III, we present the predictions to the branching fractions for various  $\Upsilon$  decays to double charmonium, and conclude that the discovery potential of these decay modes is promising in the prospective Super  $B$  experiment. We also discuss the relative phases among three amplitudes, putting particular emphasis on the nearly orthogonal relative phase between strong and electromagnetic amplitudes. The connection between our results and the previous discussions on the nearly  $90^\circ$  relative phase in  $J/\psi$  decays is remarked. In addition, we also study the impact of the resonance-continuum interference on  $J/\psi + \eta_c$  production cross sections at various  $\Upsilon$  resonances in  $e^+e^-$  experiments. We summarize and give a brief outlook in Section IV. In the Appendixes, we illustrate how to analytically derive some loop integrals that appear in Section II.

## II. COLOR-SINGLET MODEL CALCULATION

The process  $\Upsilon \rightarrow J/\psi + \eta_c$  can proceed via three stages: the  $b\bar{b}$  pair first annihilates into three gluons, or two gluons plus a photon, or a single photon; in the second step, these highly virtual gluons/photon then convert into two  $c\bar{c}$  pairs, which finally materialize into two fast-moving  $S$ -wave charmonium states. Due to the heavy charm and even much heavier bottom, both the annihilation of  $b\bar{b}$  and creations of  $c\bar{c}$  pairs take place in rather short distances, it is thereby appropriate to utilize pQCD to study this hard exclusive process.

This process is somewhat similar to the widely studied  $J/\psi \rightarrow PV$  decay, but bears the virtue that applicability of pQCD should be more reliable. It is commonly believed that some nonperturbative mechanisms should play a dominate role in many charmonium exclusive decay processes, where the credence of pQCD seems rather questionable. This consensus is exemplified by the notorious  $\rho\pi$  puzzle [2, 18].

While it is customary to use the light-cone approach to deal with hard exclusive processes involving light mesons (for a recent attempt to study  $J/\psi \rightarrow \rho\pi$  from this perspective, see Ref. [19]), it is for our purpose most proper to employ an approach embodying the non-relativistic nature of quarkonium. *NRQCD factorization* is a widely accepted effective-field-theory framework to describe the quarkonium inclusive production and decay processes, which incorporates systematically the small velocity expansion [3]. Although a rigorous formulation for exclusive quarkonium decay has not yet been fully achieved within this scheme, one may still be well motivated to work with models akin to the NRQCD ansatz.

The *color-singlet model* can be viewed as a truncated version of NRQCD approach, in which one still assumes a factorization formula, *i.e.*, the decay rate can be separated into the perturbatively calculable part and universal nonperturbative factors, however only with the contribution from the color-singlet channel retained. We do not know how to include the possible color-octet contributions in a clear-cut way, but it is plausible to assume their effects are unimportant for reactions involving only  $S$ -wave quarkonium as in our case. Notice that NRQCD and color-singlet model are often referring to the same tool in literature, so we will also use them interchangeably.

Let  $Q$ ,  $P$  and  $\tilde{P}$  signify the momenta of  $\Upsilon$ ,  $J/\psi$  and  $\eta_c$ , respectively. In color-singlet model calculation, one starts with the parton process  $b(p_b)\bar{b}(p_{\bar{b}}) \rightarrow c(p_c)\bar{c}(p_{\bar{c}}) + c(\tilde{p}_c)\bar{c}(\tilde{p}_{\bar{c}})$ , then projects this matrix element onto the corresponding color-singlet quarkonium Fock states. This work is intended only for the zeroth order in relativistic expansion, hence we can neglect the relative momenta inside each quarkonium, *i.e.*, set  $p_b = p_{\bar{b}} = Q/2$ ,  $p_c = p_{\bar{c}} = P/2$ , and  $\tilde{p}_c = \tilde{p}_{\bar{c}} = \tilde{P}/2$ . For the  $b\bar{b}$  pair to be in a spin-triplet and color-singlet state, one simply

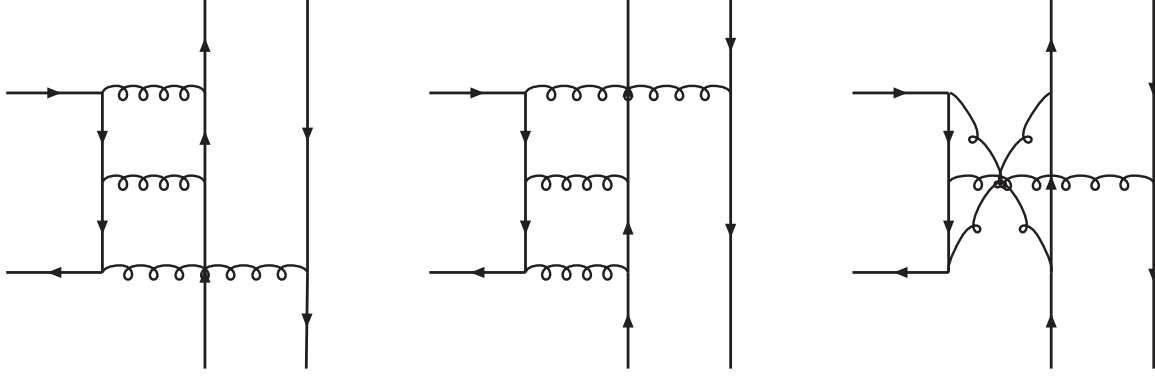


FIG. 1: Some representative lowest-order diagrams that contribute to  $\Upsilon \rightarrow 3g \rightarrow J/\psi + \eta_c$ .

replaces the product of the Dirac and color spinors for  $b$  and  $\bar{b}$  by the projection operator

$$u(p_b) \bar{v}(p_{\bar{b}}) \longrightarrow \frac{1}{2\sqrt{2}} (\not{Q} + 2m_b) \not{\epsilon}_\Upsilon \times \left( \frac{1}{\sqrt{m_b}} \psi_\Upsilon(0) \right) \otimes \frac{\mathbf{1}_c}{\sqrt{N_c}}. \quad (2)$$

For the outgoing  $J/\psi$  and  $\eta_c$ , one makes the following replacements:

$$v(p_{\bar{c}}) \bar{u}(p_c) \longrightarrow \frac{1}{2\sqrt{2}} \not{\epsilon}_{J/\psi}^* (\not{P} + 2m_c) \times \left( \frac{1}{\sqrt{m_c}} \psi_{J/\psi}(0) \right) \otimes \frac{\mathbf{1}_c}{\sqrt{N_c}}, \quad (3)$$

$$v(\tilde{p}_{\bar{c}}) \bar{u}(\tilde{p}_c) \longrightarrow \frac{1}{2\sqrt{2}} i\gamma_5 (\not{\tilde{P}} + 2m_c) \times \left( \frac{1}{\sqrt{m_c}} \psi_{\eta_c}(0) \right) \otimes \frac{\mathbf{1}_c}{\sqrt{N_c}}. \quad (4)$$

Here  $\varepsilon_\Upsilon^\mu$  and  $\varepsilon_{J/\psi}^\mu$  are polarization vectors for  $\Upsilon$  and  $J/\psi$ .  $N_c = 3$ , and  $\mathbf{1}_c$  stands for the unit color matrix. The nonperturbative factors  $\psi_\Upsilon(0)$ ,  $\psi_{J/\psi}(0)$  and  $\psi_{\eta_c}(0)$  are Schrödinger wave functions at the origin for  $\Upsilon$ ,  $J/\psi$  and  $\eta_c$ , which can be inferred either from phenomenological potential models or extracted from experiments. By writing (2), (3) and (4) the way as they are, it is understood that  $M_\Upsilon = 2m_b$  and  $M_{J/\psi} \approx M_{\eta_c} = 2m_c$  have been assumed.

Before moving into the concrete calculation, we recall first that since both strong and electromagnetic interactions conserve parity, the decay amplitude is then constrained to have the following Lorentz structure:

$$\mathcal{M} = \mathcal{A} \epsilon_{\mu\nu\alpha\beta} \varepsilon_\Upsilon^\mu \varepsilon_{J/\psi}^{*\nu} Q^\alpha P^\beta. \quad (5)$$

Apparently,  $J/\psi$  must be transversely polarized in  $\Upsilon$  rest frame. All the dynamics is encoded in the coefficient  $\mathcal{A}$ , which we call *reduced* amplitude. Our task in the remaining section then is to dig out its explicit form.

### A. Three-gluon Amplitude

We begin with the strong decay amplitude. Some typical lowest-order diagrams are shown in Fig. 1, which starts already at one loop order. Using the projection operators in (2), (3),

and (4), we can write down the corresponding amplitude:

$$\begin{aligned}
\mathcal{M}_{3g} = & 2 N_c^{-3/2} \text{tr}(T^a T^b T^c) \text{tr}(T^a \{T^b, T^c\}) g_s^6 \frac{\psi_\Upsilon(0) \psi_{J/\psi}(0) \psi_{\eta_c}(0)}{16\sqrt{2} m_b^{7/2} m_c} \int \frac{d^4 k_1}{(2\pi)^4} \frac{1}{k_1^2} \frac{1}{k_2^2} \\
& \times \left\{ \frac{\text{tr}[(\not{Q} + 2m_b) \not{\Upsilon} \gamma^\rho \gamma^\nu (\not{k}_2 + m_b) \gamma^\mu]}{k_2^2 - m_b^2} + \frac{\text{tr}[(\not{Q} + 2m_b) \not{\Upsilon} \gamma^\nu (-\not{k}_1 + m_b) \gamma^\mu \gamma^\rho]}{k_1^2 - m_b^2} \right. \\
& \left. - \frac{m_b \text{tr}[\not{Q} + 2m_b) \not{\Upsilon} \gamma^\mu (-\not{k}_2 + m_b) \gamma^\rho (\not{k}_1 + m_b) \gamma^\nu]}{(k_1^2 - m_b^2)(k_2^2 - m_b^2)} \right\} \\
& \times \frac{\text{tr}[\not{\epsilon}_{J/\psi}^* (\not{P} + 2m_c) \gamma_\mu (\not{p}_c - \not{k}_1 + m_c) \gamma_\nu \gamma_5 (\not{\tilde{P}} + 2m_c) \gamma_\rho]}{(p_c - k_1)^2 - m_c^2}, \tag{6}
\end{aligned}$$

where two internal gluons carry momenta  $k_1$  and  $k_2$ , respectively, which are subject to the constraint  $k_1 + k_2 = \frac{Q}{2}$ . Some elaboration is in order. Because  $\Upsilon$  has charge conjugation quantum number  $-1$ , three intermediate gluons must arrange to the color-singlet state  $d^{abc}|a\rangle|b\rangle|c\rangle$  [ $d^{abc}(f^{abc})$  represents the totally (anti)symmetric structure constants of  $SU(N_c)$  group]. This restriction removes all the possible  $\mathcal{O}(g_s^6)$  diagrams involving 3-gluon vertex. As a result, we only need retain those Abelian diagrams in which each of three gluons is connected between the  $b$  and  $c$  quark lines in both ends. There are totally twelve such diagrams, but it turns out that for each of diagrams, there is another one generating exactly identical amplitude, which explains the prefator 2 in the right hand side of (6). Among the six diagrams needed to be considered, one can further divide them into two groups: one carries a color factor  $\propto \text{tr}(T^a T^b T^c) \text{tr}(T^a T^c T^b)$ , whereas the other carries that  $\propto \text{tr}(T^a T^b T^c) \text{tr}(T^a T^b T^c)$ . These two groups yield identical reduced amplitudes except this difference. Thus we only need consider three diagrams with distinct topologies, as depicted in Fig. 1, and incorporate the following color factor:

$$\text{tr}(T^a T^b T^c) \text{tr}(T^a \{T^b, T^c\}) = \frac{1}{8} d_{abc} d^{abc} = \frac{(N_c^2 - 1)(N_c^2 - 4)}{8N_c}, \tag{7}$$

which reassures us that only those intermediate gluons with overall  $C = -1$  can contribute to this process.

Straightforward power counting reveals that the loop integrals in (6) are simultaneously ultraviolet and infrared finite. In absence of the need for regularization, we have directly put the spacetime dimension to four.

After completing the Dirac trace in (6), we end up with terms in which the Levi-Civita tensor is entangled with the loop momentum variable. Since all these terms will finally conspire to arrive at the desired Lorentz structure as dictated in (5), we may exploit this knowledge to get rid of the antisymmetric tensor prior to performing the loop integral [20]. First we may identify the partial amplitude  $M_{\mu\nu}$  through  $\mathcal{M} = M_{\mu\nu} \varepsilon_\Upsilon^\mu \varepsilon_{J/\psi}^{*\nu}$ . Equation (5) then demands

$$M_{\mu\nu} = \mathcal{A} \epsilon_{\mu\nu\alpha\beta} Q^\alpha P^\beta, \tag{8}$$

Contracting both sides of (8) with  $\epsilon^{\mu\nu\rho\sigma} Q_\rho P_\sigma$ , one can extract the reduced amplitude using

$$\mathcal{A} = \frac{1}{2M_\Upsilon^2 |\mathbf{P}|^2} \epsilon^{\mu\nu\rho\sigma} M_{\mu\nu} Q_\rho P_\sigma, \tag{9}$$

where  $|\mathbf{P}| = [(Q \cdot P)^2 - Q^2 P^2]^{1/2}/M_\Upsilon$  is the modulus of the momentum of  $J/\psi$  ( $\eta_c$ ) in the  $\Upsilon$  rest frame.

After this manipulation is done, we end in a concise expression

$$\mathcal{A}_{3g} = \frac{2\sqrt{2}(N_c^2 - 1)(N_c^2 - 4)}{N_c^{5/2}} \frac{\pi \alpha_s^3}{m_b^{7/2} |\mathbf{P}|^2} \psi_\Upsilon(0) \psi_{J/\psi}(0) \psi_{\eta_c}(0) f\left(\frac{m_c^2}{m_b^2}\right), \quad (10)$$

where  $f = f_1 + f_2 + f_3$ , and

$$f_1 = \int \frac{d^4 k_1}{i\pi^2} \frac{(m_b^2 - 4m_c^2)(k_2^2 - m_b^2) + k_1 \cdot (3Q - P) k_1 \cdot P - (1 + m_c^2/m_b^2)(k_1 \cdot Q)^2}{k_1^2 k_2^2 (k_2^2 - m_b^2) (k_1^2 - k_1 \cdot P)}, \quad (11)$$

$$f_2 = \int \frac{d^4 k_1}{i\pi^2} \frac{(m_b^2 - 4m_c^2)(k_1^2 - m_b^2) + k_2 \cdot P k_2 \cdot \tilde{P} - (m_c^2/m_b^2)(k_2 \cdot Q)^2}{k_1^2 (k_1^2 - m_b^2) k_2^2 (k_1^2 - k_1 \cdot P)}, \quad (12)$$

$$f_3 = m_b^2 \int \frac{d^4 k_1}{i\pi^2} \frac{k_1 \cdot (Q - 2P)(k_1^2 - k_1 \cdot \tilde{P}) - 2(m_b^2 - 4m_c^2)k_1 \cdot k_2}{k_1^2 (k_1^2 - m_b^2) k_2^2 (k_2^2 - m_b^2) (k_1^2 - k_1 \cdot P)}. \quad (13)$$

Since  $f_i$  is dimensionless, it can depend upon  $m_b$  and  $m_c$  only through their dimensionless ratio  $m_c^2/m_b^2$ . These loop integrals can be worked out analytically, and the results are

$$\begin{aligned} \text{Re } f(\xi) = & 3 - \frac{2\pi}{\sqrt{3}} + 4(1 - 2\xi) \left\{ \frac{1}{1 - \beta} \ln \left[ \frac{1 + \beta}{2} \right] + \frac{1}{1 + \beta} \ln \left[ \frac{1 - \beta}{2} \right] \right\} \\ & - 2(1 + 2\xi) \left\{ \frac{1}{(1 - \beta)^2} \ln \left[ \frac{1 + \beta}{2} \right] + \frac{1}{(1 + \beta)^2} \ln \left[ \frac{1 - \beta}{2} \right] + \frac{1}{4\xi} \right\} \\ & - \frac{1 - 2\xi}{\beta} \left\{ 2 \tanh^{-1} \beta \ln \xi + 2 \text{Li}_2 \left[ \frac{1 - \beta}{2} \right] - 2 \text{Li}_2 \left[ \frac{1 + \beta}{2} \right] + \text{Li}_2 \left[ \frac{\beta - 1}{\beta + 1} \right] \right. \\ & \left. - \text{Li}_2 \left[ \frac{\beta + 1}{\beta - 1} \right] \right\} + \frac{4\xi}{\beta} \left\{ \frac{2\pi}{3} \tan^{-1}[\sqrt{3}\beta] + 2 \tanh^{-1} \beta \ln[1 - 3\xi] \right. \\ & + \text{Li}_2 \left[ \frac{2\beta}{1 + \beta} \right] - \text{Li}_2 \left[ \frac{2\beta}{\beta - 1} \right] + \text{Li}_2 \left[ \frac{\beta(\beta + 1)}{\beta - 1} \right] - \text{Li}_2 \left[ \frac{\beta(1 - \beta)}{1 + \beta} \right] \\ & + \text{Li}_2 \left[ \frac{\beta(1 + \beta)}{2(1 - 3\xi)} \right] - \text{Li}_2 \left[ \frac{\beta(\beta - 1)}{2(1 - 3\xi)} \right] + \text{Li}_2 \left[ -\frac{\beta(1 - \beta)^2}{4(1 - 3\xi)} \right] - \text{Li}_2 \left[ \frac{\beta(1 + \beta)^2}{4(1 - 3\xi)} \right] \\ & \left. + 2 \text{Re} \left\{ \text{Li}_2 \left[ -\frac{(1 + i\sqrt{3})\beta}{1 - i\sqrt{3}\beta} \right] - \text{Li}_2 \left[ \frac{(1 + i\sqrt{3})\beta}{1 + i\sqrt{3}\beta} \right] \right\} \right\}, \quad (14) \end{aligned}$$

$$\text{Im } f(\xi) = \pi \left\{ 1 - \frac{2(1 - 2\xi) \tanh^{-1} \beta}{\beta} \right\}, \quad (15)$$

where  $\text{Li}_2$  is the dilogarithm function, and  $\beta = \sqrt{1 - 4\xi}$ . We will illustrate in Appendix A how to obtain this result. The emergence of imaginative part of  $f$  characterizes the contribution from two on-shell internal gluons. The shapes of the real and imaginary parts of  $f$  are displayed in Fig. 3.

It is instructive to know the asymptotic behavior of  $f$  in the  $\xi \rightarrow 0$  limit. This can be readily read out from (14) and (15),

$$\text{Re } f(\xi) = \frac{1}{2} \ln^2 \xi + \frac{3}{2} \ln \xi + 1 + \frac{\pi^2}{6} - \frac{2\pi}{\sqrt{3}} + \mathcal{O}(\xi \ln \xi), \quad (16)$$

$$\text{Im } f(\xi) = \pi (\ln \xi + 1) + \mathcal{O}(\xi \ln \xi). \quad (17)$$

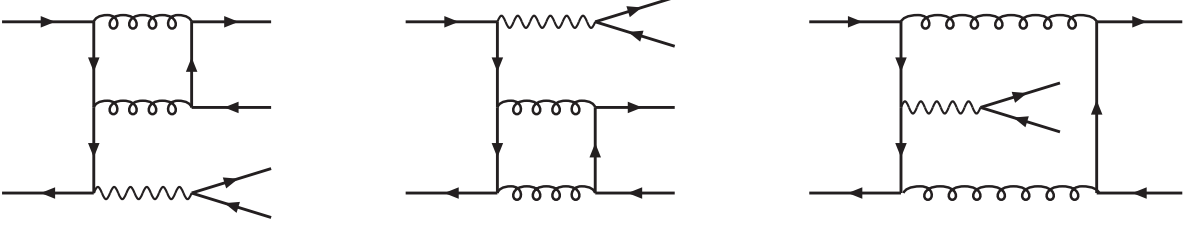


FIG. 2: Three representative lowest-order diagrams that contribute to  $\Upsilon \rightarrow gg\gamma \rightarrow J/\psi + \eta_c$ , where the  $J/\psi$  comes from the photon fragmentation.

Note both the real and imaginary parts blow up logarithmically in the limit  $\xi \rightarrow 0$ , as can be clearly visualized in Fig. 3. These (quadratically) logarithmical divergences in the  $m_c \rightarrow 0$  limit are obviously of infrared origin. Nevertheless, this does not pose any practical problem, since a nonrelativistic description for a zero-mass bound state, as well as the resulting predictions, should not be trusted anyway. It is interesting to note that, provided that  $\xi$  is not overly small, say,  $\xi > 10^{-4}$ , then  $-\text{Im } f$  is always bigger than  $|\text{Re } f|$ , or more precisely phrased,  $-\frac{3\pi}{4} < \arg f < -\frac{\pi}{4}$ .

## B. Two-gluon-one-photon Amplitude

We next turn to the contribution through the radiative decay channel.  $C$ -parity conservation demands that one end of photon line must be attached to the  $b$  quark. Those diagrams obtained from replacing one gluon by one photon in Fig. 1 do contribute, however their magnitudes are much less important than the diagrams shown in Fig. 2, which essentially proceed as  $\Upsilon \rightarrow gg(\rightarrow \eta_c) + \gamma(\rightarrow J/\psi)$ . This is because in the latter case, the  $J/\psi$  is created via the photon fragmentation, which thereby receives a  $m_b^2/m_c^2$  enhancement relative to the former. We will only consider the latter case, in which the lowest-order contribution also starts at one loop. Using the projection operators in (2), (3), and (4), it is straightforward to write down the corresponding amplitude:

$$\begin{aligned}
\mathcal{M}_{gg\gamma} = & 2 N_c^{-1/2} \text{tr}(T^a T^b) \text{tr}(T^a T^b) e_b e_c e^2 g_s^4 \frac{\psi_\Upsilon(0) \psi_{J/\psi}(0) \psi_{\eta_c}(0)}{8\sqrt{2} m_b^{1/2} m_c^2} \int \frac{d^4 k_1}{(2\pi)^4} \frac{1}{k_1^2} \frac{1}{k_2^2} \\
& \times \left\{ \frac{\text{tr}[(\not{Q} + 2m_b) \not{\epsilon}_\Upsilon \not{\epsilon}_{J/\psi}^* (\not{P} - \not{p}_b + m_b) \gamma^\nu (\not{p}_b - \not{k}_1 + m_b) \gamma^\mu]}{((P - p_b)^2 - m_b^2)((p_b - k_1)^2 - m_b^2)} \right. \\
& + \frac{\text{tr}[(\not{Q} + 2m_b) \not{\epsilon}_\Upsilon \gamma^\nu (\not{k}_2 - \not{p}_b + m_b) \gamma^\mu (\not{p}_b - \not{P} + m_b) \not{\epsilon}_{J/\psi}^*]}{((P - p_b)^2 - m_b^2)((p_b - k_2)^2 - m_b^2)} \\
& + \left. \frac{\text{tr}[(\not{Q} + 2m_b) \not{\epsilon}_\Upsilon \gamma^\nu (\not{k}_2 - \not{p}_b + m_b) \not{\epsilon}_{J/\psi}^* (\not{p}_b - \not{k}_1 + m_b) \gamma^\mu]}{((p_b - k_1)^2 - m_b^2)((p_b - k_2)^2 - m_b^2)} \right\} \\
& \times \frac{\text{tr}[\gamma_5 (\tilde{\not{P}} + 2m_c) \gamma_\mu (\not{p}_c - \not{k}_1 + m_c) \gamma_\nu]}{(\tilde{p}_c - k_1)^2 - m_c^2}, \tag{18}
\end{aligned}$$

where the momenta carried by two internal gluons are labelled by  $k_1, k_2$ , which satisfy  $k_1 + k_2 = \tilde{P}$ . The factor 2 in the right side of (18) takes into account the identical contributions

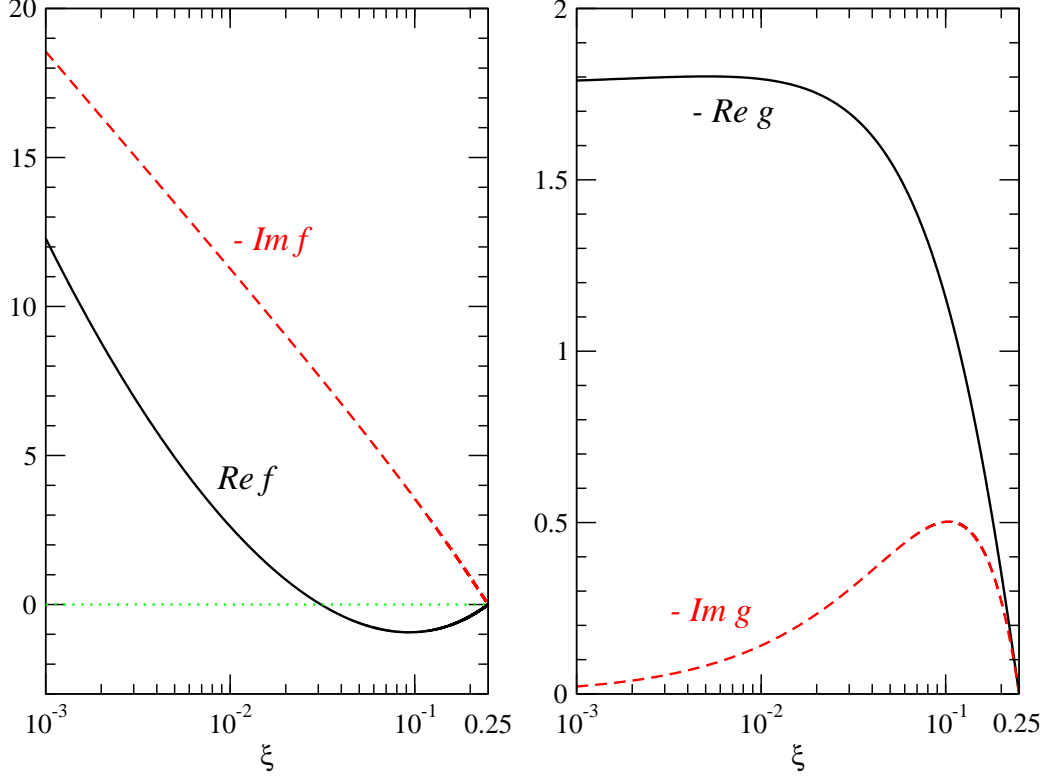


FIG. 3: Real and imaginary parts of  $f(\xi)$  and  $g(\xi)$ .

from other three crossed diagrams.

Following the same shortcut adopted in the  $3g$  channel, we can derive the desired reduced amplitude with recourse to Eq. (9),

$$\mathcal{A}_{gg\gamma} = \frac{4\sqrt{2}(N_c^2 - 1)}{N_c^{1/2}} \frac{e_b e_c \pi \alpha \alpha_s^2 m_b^{1/2}}{(m_b^2 - 2m_c^2) |\mathbf{P}|^2 m_c^2} \psi_\Upsilon(0) \psi_{J/\psi}(0) \psi_{\eta_c}(0) g\left(\frac{m_c^2}{m_b^2}\right), \quad (19)$$

where the dimensionless function  $g$  is defined by

$$g\left(\frac{m_c^2}{m_b^2}\right) = \int \frac{d^4 k_1}{i\pi^2} \frac{(2m_c^2/m_b^2 Q \cdot r - P \cdot r) \tilde{P} \cdot r + 2(m_b^2 - 4m_c^2) r^2}{k_1^2 k_2^2 (k_1^2 - k_1 \cdot Q)(k_2^2 - k_2 \cdot Q)}. \quad (20)$$

For convenience, we have introduced a new internal momentum variable  $r$ , which is defined through  $k_1 = \tilde{P}/2 + r$  and  $k_2 = \tilde{P}/2 - r$ . Note that the integrand is symmetric under  $r \rightarrow -r$ , reflecting the symmetry  $k_1 \leftrightarrow k_2$ . A gratifying fact is that the charm propagator has now been cancelled in the denominator. We dedicate Appendix B to a detailed derivation of this loop integral. Like its counterpart  $f$  in the three-gluon channel, the function  $g$  is both



ultraviolet and infrared finite. Its analytic expression reads

$$\begin{aligned}
\text{Re } g(\xi) = & (1 - 2\xi) \ln[2 - 4\xi] + 4\sqrt{\xi(1 - \xi)} \tan^{-1} \sqrt{\frac{\xi}{1 - \xi}} \\
& - \xi\beta \left\{ 4 \tanh^{-1}\beta \ln[2\xi] + 2 \text{Li}_2[-\beta] - 2 \text{Li}_2[\beta] + \text{Li}_2 \left[ \frac{\beta - 1}{\beta + 1} \right] \right. \\
& - \text{Li}_2 \left[ \frac{\beta + 1}{\beta - 1} \right] + \text{Li}_2 \left[ \frac{2\beta}{(1 + \beta)^2} \right] - \text{Li}_2 \left[ -\frac{2\beta}{(1 - \beta)^2} \right] \left. \right\} \\
& - \frac{(1 - 2\xi)^2}{\beta} \left\{ \text{Li}_2[\beta] - \text{Li}_2[-\beta] + 2 \text{Re} \left\{ \text{Li}_2 \left[ \frac{(1 + \beta)^2 + 4i\sqrt{\xi(1 - \xi)}}{4(1 - 2\xi)} \right] \right. \right. \\
& - \text{Li}_2 \left[ \frac{(1 - \beta)^2 + 4i\sqrt{\xi(1 - \xi)}}{4(1 - 2\xi)} \right] + \text{Li}_2 \left[ -\frac{\beta(1 - \beta)^2 + 4i\beta\sqrt{\xi(1 - \xi)}}{4(1 - 2\xi)} \right] \\
& \left. \left. - \text{Li}_2 \left[ \frac{\beta(1 + \beta)^2 + 4i\beta\sqrt{\xi(1 - \xi)}}{4(1 - 2\xi)} \right] \right\} \right\}, \tag{21}
\end{aligned}$$

$$\text{Im } g(\xi) = -2\pi \xi\beta \tanh^{-1}\beta. \tag{22}$$

The shapes of real and imaginary parts of  $g$  are displayed in Fig. 3. Note that  $-\text{Re } g$  is always bigger than  $-\text{Im } g$  for any  $\xi$ , or put in another way,  $-\pi < \arg g < -\frac{3\pi}{4}$ . Apparently, the imaginary part of  $g$  vanishes as  $\xi \rightarrow 0$ , whereas the real part of  $g$  approaches the following asymptotic value:

$$\text{Re } g(\xi) = -\frac{\pi^2}{4} + \ln 2 + \mathcal{O}(\xi \ln \xi). \tag{23}$$

In contrast to  $f$ , both of the real and imaginary parts of  $g$  admit a finite value in the  $\xi \rightarrow 0$  limit. Not surprisingly, the asymptotic behavior of this function is quite similar to the analogous one in the  $\Upsilon \rightarrow \eta_c \gamma$  process [20].

### C. Single-photon Amplitude

Let us now consider the electromagnetic contribution via the annihilation of  $b\bar{b}$  into a single photon, with some typical diagrams shown in Fig. 4. This process is closely related to the continuum  $J/\psi + \eta_c$  production in  $e^+e^-$  annihilation, which has recently aroused much attention since the measurements were first released by Belle collaboration [11]. Rather unexpectedly, it is shortly found that the leading-order NRQCD prediction to the production cross section falls short of the data by about one order of magnitude [21, 22], which subsequently triggered intensive theoretical efforts to resolve this alarming discrepancy [23, 24, 25, 26, 27, 28, 29, 30].

In the Born order, one can directly import the time-like electromagnetic form factor of  $S$ -wave charmonium first deduced in Ref. [21] to here, and the corresponding lowest-order one-photon amplitude reads

$$\mathcal{A}_\gamma = -\frac{16\sqrt{2}(N_c^2 - 1)}{N_c^{1/2}} \frac{\pi^2 e_b e_c \alpha \alpha_s}{m_b^{11/2}} \psi_\Upsilon(0) \psi_{J/\psi}(0) \psi_{\eta_c}(0) \left( 1 + \frac{N_c^2}{2(N_c^2 - 1)} \frac{e_c^2 \alpha m_b^2}{\alpha_s m_c^2} \right), \tag{24}$$

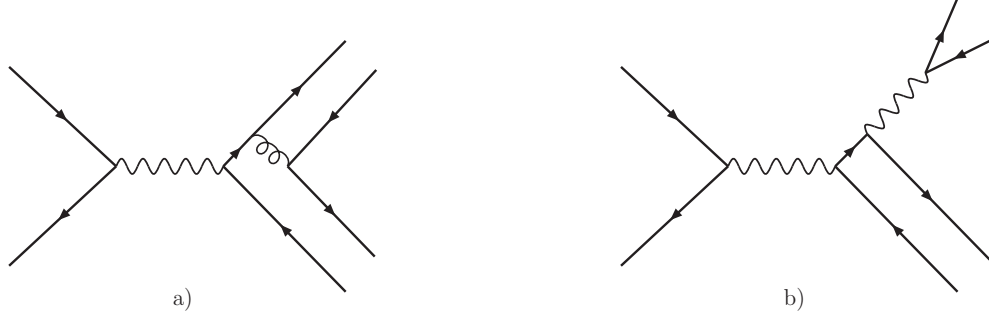


FIG. 4: Two representative lowest-order diagrams that contribute to  $\Upsilon \rightarrow \gamma^* \rightarrow J/\psi + \eta_c$ . There are totally four diagrams in class a) and two in class b).

where the second term in the parenthesis represents the pure QED contribution in which  $J/\psi$  arises from photon fragmentation, as is represented by Fig. 4b).

Recent calculations indicate that the  $J/\psi + \eta_c$  electromagnetic form factor is subject to large perturbative and relativistic corrections at  $B$  factory energy [28, 30]. It seems that the disturbing discrepancy between  $B$  factories measurements and NRQCD predictions have been largely resolved once these large corrections are taken into account. Motivated by this, from now on we will replace the entities in the parenthesis in (24) by a positive constant  $K$  ( $> 1$ ), which presumably encompasses all the radiative and relativistic corrections.

#### D. Decay Width and Asymptotic Scaling Behavior

It is now the time to lump three different contributions together. Plugging (10), (19), and (24) into the formula

$$\Gamma[\Upsilon \rightarrow J/\psi + \eta_c] = \frac{|\mathbf{P}|^3}{12\pi} |\mathcal{A}_\gamma + \mathcal{A}_{3g} + \mathcal{A}_{gg\gamma}|^2, \quad (25)$$

we then obtain the desired decay partial width. Note the cubic power of momentum reflects that  $J/\psi$  and  $\eta_c$  are in relative  $P$  wave. This formula has already taken into account the spin average of  $\Upsilon$  and the polarization sum over  $J/\psi$ . The result is

$$\begin{aligned} \Gamma[\Upsilon \rightarrow J/\psi + \eta_c] &= \Gamma[\Upsilon \rightarrow e^+e^-] \\ &\times \frac{2^{20} \pi^2 e_c^2 \alpha_s^2 |\mathbf{P}|^3}{9 M_\Upsilon^9} \psi_{J/\psi}^2(0) \psi_{\eta_c}^2(0) |a_\gamma + a_{3g} + a_{gg\gamma}|^2, \end{aligned} \quad (26)$$

where  $a_\gamma = K$ ,

$$a_{3g} = -\frac{5 \alpha_s^2}{72\pi e_b e_c \alpha} \frac{m_b^2}{|\mathbf{P}|^2} f\left(\frac{m_c^2}{m_b^2}\right), \quad (27)$$

$$a_{gg\gamma} = -\frac{\alpha_s}{4\pi} \frac{m_b^6}{(m_b^2 - 2m_c^2)|\mathbf{P}|^2 m_c^2} g\left(\frac{m_c^2}{m_b^2}\right), \quad (28)$$

and  $\Gamma[\Upsilon \rightarrow e^+e^-] = 16\pi e_b^2 \alpha^2 \psi_\Upsilon^2(0)/M_\Upsilon^2$  is the electronic width of  $\Upsilon$ .

It is instructive to deduce the asymptotic behaviors of these three different contributions. Because we are more concerned about the power-law scaling, we will take  $f, g \sim \mathcal{O}(1)$  for simplicity since they vary with quark masses logarithmically at most. Assuming  $\psi_{J/\psi}(0) \sim \psi_{\eta_c}(0) \sim (m_c v_c)^{3/2}$  ( $v_c$  is the typical relative velocity between  $c$  and  $\bar{c}$ ), from (26) we find

$$\frac{\Gamma[\Upsilon \rightarrow \gamma^* \rightarrow J/\psi + \eta_c]}{\Gamma[\Upsilon \rightarrow e^+ e^-]} \sim \alpha_s^2 \frac{m_c^6}{m_b^6} v_c^6, \quad (29)$$

$$\frac{\Gamma[\Upsilon \rightarrow 3g \rightarrow J/\psi + \eta_c]}{\Gamma[\Upsilon \rightarrow e^+ e^-]} \sim \frac{\alpha_s^6}{\alpha^2} \frac{m_c^6}{m_b^6} v_c^6, \quad (30)$$

$$\frac{\Gamma[\Upsilon \rightarrow gg\gamma \rightarrow J/\psi + \eta_c]}{\Gamma[\Upsilon \rightarrow e^+ e^-]} \sim \alpha_s^4 \frac{m_c^2}{m_b^2} v_c^6. \quad (31)$$

First interesting observation is that both (29) and (30) exhibit the  $1/m_b^6$  scaling behavior. This is as expected from the celebrated helicity selection rule in perturbative QCD, which is applicable for both single-photon and three-gluon processes [9]. The reason is as follows. The final-state  $J/\psi$  must be transversely polarized, in line with the parity and Lorentz invariance, the hadron helicity conservation  $\lambda_{J/\psi} + \lambda_{\eta_c} = 0$  is violated by one unit, hence the ratio is suppressed by an extra  $1/m_b^2$  relative to the leading-twist  $1/m_b^4$  scaling. In contrast, the corresponding ratio in  $gg\gamma$  channel, (31), though suppressed by coupling constants with respect to other two subprocesses, nevertheless enjoys a much milder ( $\sim 1/m_b^2$ ) kinematical suppression, because the  $J/\psi$  directly comes from the photon fragmentation. Simple power counting implies that these three different contributions have comparable strengths for the physical masses of  $b$  and  $c$ .

Another noteworthy fact is that, there are relative phases among three amplitudes, which are encoded in the  $f$  and  $g$  functions. Since all these phases originate from the loop integrals, we may regard them of short-distance origin.

### III. PHENOMENOLOGY

#### A. Determination of $K$ from $B$ factories measurement

First we want to determine the value of  $K$  in (26), which characterizes the magnitude of higher-order corrections to the single-photon amplitude. For the sake of simplicity, we will assume the  $K$  factors are equal in our case and in  $J/\psi + \eta_c$  production through  $e^+ e^-$  annihilation to a virtual photon. Of course, this is just an approximation, because the virtual gluon line connecting  $b$  quark and final-state  $c$  quark, as well as the relativistic correction in  $\Upsilon$ , which will emerge in our process accounting for the radiative and relative corrections, are absent in the double charmonium production in continuum. We will assume these additional corrections are insignificant.

First we recall the continuum double charmonium cross section in the lowest order in  $\alpha_s$  and  $v_c^2$  [21, 22]:

$$\sigma_{\text{cont}}[e^+ e^- \rightarrow J/\psi + \eta_c] = \sigma_{\mu^+ \mu^-} \frac{2^{20} \pi^2 e_c^2 \alpha_s^2 |\mathbf{P}|^3}{9 s^{9/2}} \psi_{J/\psi}^2(0) \psi_{\eta_c}^2(0), \quad (32)$$

where  $\sigma_{\mu^+ \mu^-} = \frac{4\pi\alpha^2}{3s}$ . For simplicity, the pure QED contribution where  $J/\psi$  is produced via photon fragmentation (the analogous diagram to Fig. 4b) has been neglected.

TABLE I: Experimental inputs for  $\Upsilon(nS)$  and  $S$ -wave charmonia (taken from Ref. [31]). The last column lists the wave functions at the origin for various  $S$ -wave charmonium states, retrieved from the measured electric width through (33) by assuming  $m_c = 1.5$  GeV and  $\alpha_s(2m_c) = 0.26$ .

$H$	Mass (GeV)	$\Gamma_{\text{tot}}$ (keV)	$\Gamma_{e^+e^-}$ (keV)	$\psi_H(0)$ (GeV $^{3/2}$ )
$\Upsilon(1S)$	9.460	$54.02 \pm 1.25$	$1.340 \pm 0.018$	–
$\Upsilon(2S)$	10.023	$31.98 \pm 2.63$	$0.612 \pm 0.011$	–
$\Upsilon(3S)$	10.355	$20.32 \pm 1.85$	$0.443 \pm 0.008$	–
$\Upsilon(4S)$	10.579	$20500 \pm 2500$	$0.272 \pm 0.029$	–
$J/\psi$	3.097	–	$5.55 \pm 0.14$	0.263
$\eta_c$	2.980	–	–	0.263
$\psi'$	3.686	–	$2.48 \pm 0.06$	0.176
$\eta'_c$	3.638	–	–	0.176

In this work, we extract the wave functions at the origin for vector charmonium states from their measured electric widths. We will use the formula incorporating the first order perturbative correction

$$\Gamma[J/\psi \rightarrow e^+e^-] = \frac{4\pi e_c^2 \alpha^2}{m_c^2} \psi_{J/\psi}^2(0) \left(1 - \frac{8\alpha_s(2m_c)}{3\pi}\right)^2. \quad (33)$$

Heavy quark spin symmetry is then invoked to infer the wave functions at origin for the corresponding  $^1S_0$  charmonium states. All the involved charmonium wave functions at origin are tabulated in Table I.

If we choose  $m_c = 1.5$  GeV,  $\alpha_s = 0.22$ , we then obtain from (32) the tree level continuum  $J/\psi + \eta_c$  cross section at  $\sqrt{s} = 10.58$  GeV to be 4.74 fb. This theoretical prediction can be contrasted with the most recent  $B$  factories measurements [32, 33]:

$$\begin{aligned} \sigma[e^+e^- \rightarrow J/\psi + \eta_c] \times \mathcal{B}_{>2}^{\eta_c} &= 25.6 \pm 2.8(\text{stat}) \pm 3.4(\text{syst}) \text{ fb}, & \text{Belle} \\ \sigma[e^+e^- \rightarrow J/\psi + \eta_c] \times \mathcal{B}_{>2}^{\eta_c} &= 17.6 \pm 2.8(\text{stat})_{-2.1}^{+1.5}(\text{syst}) \text{ fb}, & \text{BABAR} \end{aligned} \quad (34)$$

where  $\mathcal{B}_{>2}^{\eta_c}$  represents the branching ratio of  $\eta_c$  decay to more than 2 charged tracks, hence should be less than 1. With large uncertainties, both measurements seem to be marginally consistent with each other.

If we assume the measured  $\sigma_{\text{cont}}[e^+e^- \rightarrow J/\psi + \eta_c]$  to be 23 fb, and expect that large radiative and relativistic corrections to (32) can bring the leading-order NRQCD prediction to this value, we then require  $K = \sqrt{23/4.74} \approx 2.2$ . This  $K$  factor is roughly consistent with what is obtained through actual higher-order NRQCD calculations [28, 30]. Although we extract this constant through the  $\Upsilon(4S) \rightarrow J/\psi + \eta_c$  process, we will assume it is universal in all other double charmonium decay channels of  $\Upsilon(nS)$ .

## B. Exclusive decay of $\Upsilon(nS)$ to double $S$ -wave charmonium

To date,  $\Upsilon$  exclusive decays to double charmonium have not yet been experimentally established. To make concrete predictions from (26), we need specify the values of all the

TABLE II: Predicted partial widths and branching ratios for various decay channels of  $\Upsilon(nS)$  to vector plus pseudoscalar charmonium.

Decay channels	$\Gamma$ (eV)	$\mathcal{B}$	Decay channels	$\Gamma$ (eV)	$\mathcal{B}$
$\Upsilon(1S) \rightarrow J/\psi + \eta_c$	$0.208^{+0.302}_{-0.126}$	$3.9^{+5.6}_{-2.3} \times 10^{-6}$	$\Upsilon(2S) \rightarrow J/\psi + \eta_c$	$0.082^{+0.119}_{-0.050}$	$2.6^{+3.7}_{-1.6} \times 10^{-6}$
$\Upsilon(1S) \rightarrow J/\psi + \eta'_c$	$0.109^{+0.185}_{-0.074}$	$2.0^{+3.4}_{-1.4} \times 10^{-6}$	$\Upsilon(2S) \rightarrow J/\psi + \eta'_c$	$0.042^{+0.067}_{-0.027}$	$1.3^{+2.1}_{-0.9} \times 10^{-6}$
$\Upsilon(1S) \rightarrow \psi' + \eta_c$	$0.093^{+0.127}_{-0.054}$	$1.7^{+2.4}_{-1.0} \times 10^{-6}$	$\Upsilon(2S) \rightarrow \psi' + \eta_c$	$0.037^{+0.051}_{-0.022}$	$1.1^{+1.6}_{-0.7} \times 10^{-6}$
$\Upsilon(1S) \rightarrow \psi' + \eta'_c$	$0.045^{+0.073}_{-0.030}$	$0.8^{+1.4}_{-0.6} \times 10^{-6}$	$\Upsilon(2S) \rightarrow \psi' + \eta'_c$	$0.017^{+0.028}_{-0.011}$	$0.5^{+0.9}_{-0.4} \times 10^{-6}$
$\Upsilon(3S) \rightarrow J/\psi + \eta_c$	$0.054^{+0.079}_{-0.033}$	$2.7^{+3.9}_{-1.6} \times 10^{-6}$	$\Upsilon(4S) \rightarrow J/\psi + \eta_c$	$0.031^{+0.046}_{-0.019}$	$1.5^{+2.2}_{-0.9} \times 10^{-9}$
$\Upsilon(3S) \rightarrow J/\psi + \eta'_c$	$0.027^{+0.043}_{-0.018}$	$1.3^{+2.1}_{-0.9} \times 10^{-6}$	$\Upsilon(4S) \rightarrow J/\psi + \eta'_c$	$0.015^{+0.025}_{-0.010}$	$0.7^{+1.2}_{-0.5} \times 10^{-9}$
$\Upsilon(3S) \rightarrow \psi' + \eta_c$	$0.024^{+0.034}_{-0.014}$	$1.2^{+1.7}_{-0.7} \times 10^{-6}$	$\Upsilon(4S) \rightarrow \psi' + \eta_c$	$0.014^{+0.019}_{-0.008}$	$0.7^{+1.0}_{-0.4} \times 10^{-9}$
$\Upsilon(3S) \rightarrow \psi' + \eta'_c$	$0.011^{+0.018}_{-0.007}$	$0.6^{+0.9}_{-0.4} \times 10^{-6}$	$\Upsilon(4S) \rightarrow \psi' + \eta'_c$	$0.007^{+0.010}_{-0.004}$	$0.3^{+0.5}_{-0.2} \times 10^{-9}$

input parameters. We fix  $m_c$  to be 1.5 GeV, but take  $m_b$  as a variable— for each  $\Upsilon(nS)$  decay process, we approximate it as half of  $M_{\Upsilon(nS)}$ . The magnitude of  $|\mathbf{P}|$  is determined by physical kinematics. We assume  $K = 2.2$  for all decay channels, and take the values of the wave functions at the origin for various charmonium from Table I. As for the coupling constants, we take  $\alpha = 1/137$ , and  $\alpha_s(m_b) = 0.22$ . The uncertainties of our predictions are estimated by sliding the renormalization scale from  $2m_b$  to  $m_b/2$  (corresponding to varying  $\alpha_s$  from 0.18 to 0.26). It should be cautioned that the ambiguity of the inputted  $b$  mass, especially for higher  $\Upsilon$  excitations, can bring even more severe uncertainty due to the higher powers of  $m_b$  appearing in (26).

Our predictions to the partial widths and branching ratios for all decay channels are listed in Table II. One clearly sees that the branching fractions for all decay processes (except for  $\Upsilon(4S)$ ) are about  $10^{-6}$ , which are perfectly compatible with the measured inclusive  $J/\psi$  production rates from  $\Upsilon(nS)$  decay, Eq. (1). It is interesting to note that our hadronic decay processes have even smaller branching ratios than the radiative decay  $\Upsilon \rightarrow \eta_c \gamma$  ( $\mathcal{B} \approx 3 \times 10^{-5}$ ) [20]. This may be partly understood by that  $\Gamma[\Upsilon \rightarrow \eta_c \gamma]/\Gamma[\Upsilon \rightarrow e^+ e^-] \sim \frac{\alpha_s^4}{\alpha} \frac{m_c^2}{m_b^2} v_c^3$ , which has a milder  $1/m_b^2$  scaling behavior compared to the  $1/m_b^6$  suppression in our processes, as manifested in Eqs. (29) and (30).

Between 2000 and 2003, CLEOIII has recorded about 20 million, 10 million and 5 million decays of  $\Upsilon(1S)$ ,  $\Upsilon(2S)$  and  $\Upsilon(3S)$ , respectively [8]. So there should be a few to tens of produced events for each double charmonium mode. Unfortunately, because the cleanest way of tagging  $J/\psi$  is through the dimuon mode, only 6% fraction of the produced events can be reconstructed. Further taking into account the acceptance and efficiency to detect  $\mu$ , it seems rather difficult to observe these double charmonium production events based on the existing CLEOIII data sample. By contrast, the high luminosity  $e^+e^-$  colliders such as Belle and BABAR have already collected a enormous amount of data at  $\Upsilon(4S)$  peak. If they could dedicate some significant period of run at the lower  $\Upsilon$  resonances, it is feasible for them to discover these decay channels unambiguously. Needless to say, the discovery potential is very promising for the planned super-high-luminosity  $e^+e^-$  facility like Super  $B$  factory.

It is important to understand the interference pattern among three different amplitudes.

In our case, the phase in each amplitude manifests itself as short-distance effect arising from loop, and is perturbatively calculable. Let us take  $\Upsilon(1S) \rightarrow J/\psi + \eta_c$  as an example. Taking  $\xi = 4m_c^2/M_\Upsilon^2 \approx 0.10$  and  $\alpha_s = 0.22$ , we find from (27) and (28)

$$a_{3g} = 3.89 e^{-i105^\circ}, \quad a_{gg\gamma} = 0.44 e^{i24^\circ}. \quad (35)$$

Curiously, the strong decay amplitude is almost orthogonal to the electromagnetic amplitude, while the radiative decay amplitude is almost in phase with the electromagnetic one. It is also obvious to see that the strong decay amplitude has the most prominent strength, the electromagnetic one the next, and the radiative decay amplitude the least.

In digression, it may be instructive to know the relative strengths of three different channels in inclusive  $\Upsilon$  decay. From the following experimental inputs:

$$R = \frac{\Gamma[\Upsilon \rightarrow \gamma^* \rightarrow X]}{\Gamma[\Upsilon \rightarrow \mu^+ \mu^-]} = 3.56 \pm 0.07, \quad [34],$$

$$R_\mu = \frac{\Gamma[\Upsilon \rightarrow ggg]}{\Gamma[\Upsilon \rightarrow \mu^+ \mu^-]} = 39.11 \pm 0.4, \quad [35],$$

$$R_\gamma = \frac{\Gamma[\Upsilon \rightarrow gg\gamma]}{\Gamma[\Upsilon \rightarrow ggg]} = 0.027 \pm 0.003, \quad [36], \quad (36)$$

we can infer

$$\mathcal{B}[\Upsilon \rightarrow ggg] : \mathcal{B}[\Upsilon \rightarrow \gamma^* \rightarrow X] : \mathcal{B}[\Upsilon \rightarrow gg\gamma] = 82.7\% : 7.5\% : 2.2\%, \quad (37)$$

where these three branching ratios sum up to  $1 - \sum \mathcal{B}[\Upsilon \rightarrow l^+ l^-] = 92.5\%$ , as they should<sup>1</sup>. A very simple expectation is that each amplitude in an exclusive process scales with the corresponding  $\sqrt{\mathcal{B}_{\text{incl}}}$ . The relative strengths of three amplitudes in (35) roughly respect this scaling rule if one assumes  $K = 1$ . Nevertheless, the truly important point is that, the orders of strengths of three amplitudes are same for both inclusive and exclusive decays.

We can gain more intuition about the interference pattern by examining the individual contribution to the partial width. Had we retained only  $a_\gamma$  in (26), the partial width for  $\Upsilon(1S) \rightarrow J/\psi + \eta_c$  would be only 0.065 eV. If we kept  $a_{3g}$  only, the width would instead be 0.204 eV. If we include both  $a_\gamma$  and  $a_{3g}$  but discard  $a_{gg\gamma}$ , the width would become 0.210 eV, which is rather close to the full answer listed in Table II, 0.208 eV. This numerical exercise clearly corroborates our expectation about the relative importance of these three different channels.

The phase structures in (35) also hold for other decay channels of  $\Upsilon(nS)$  to double charmonium. We take  $\Upsilon(4S) \rightarrow J/\psi + \eta_c$  as second example to verify this point. Taking  $\xi = 4m_c^2/M_{\Upsilon(4S)}^2 \approx 0.08$ , we obtain

$$a_{3g} = 4.20 e^{-i102^\circ}, \quad a_{gg\gamma} = 0.52 e^{i20^\circ}. \quad (38)$$

It has been of great interest to decipher the interference pattern between the strong and electromagnetic amplitude in  $J/\psi$  decays. The relative phase between  $3g$  and  $\gamma$  amplitude in  $J/\psi \rightarrow PV$  has been determined to be around  $-(106 \pm 10)^\circ$  [12, 13, 14, 15, 16, 17]. This

---

<sup>1</sup> We have not included the contribution from the radiative transition  $\Upsilon \rightarrow \eta_b \gamma$ , which has a completely negligible branching ratio.

is surprisingly close to our finding in  $\Upsilon$  decay. Suzuki has argued that the large relative phase in  $J/\psi$  decay must arise from long-distance rescattering effect, and emphasized that it is impossible for the perturbative quark-gluon process to generate it [16]. However, our calculation provides an explicit counterexample against his claim, showing that the short-distance contribution alone suffices to generating such a large relative phase.

It is worth mentioning that some years ago, Gerard and Weyers argued there should be universal orthogonality between strong and electromagnetic amplitude for each  $J/\psi$  exclusive decay mode [37]. This assertion may seem to be backed by numerous phenomenological evidences<sup>2</sup>. They have attributed this orthogonality simply to the orthogonality of gluonic and one photon states. Inspecting their arguments carefully, one finds that they only prove the incoherence between three-gluon and single-photon decays at *inclusive* level, whose validity crucially relies on summing over all possible decay channels. Since there is no room for such a summation for exclusive  $J/\psi$  decay, there is no any simple reason to believe why strong decay amplitude should be orthogonal to the electromagnetic amplitude channel by channel.

Because their reasoning is based on rather general ground, one may test it in  $\Upsilon$  exclusive decay. As a matter of fact, we can directly present a counterexample. Imagine a fictitious world with an extremely heavy  $b$  quark, say  $m_b \sim M_{\text{Plank}}$ , but with an ordinary charm quark. For the would-be  $\Upsilon$  decay to  $J/\psi + \eta_c$ , we then find from (16) and (17) that the phase of  $f$  is very close to zero, so is the relative phase between  $a_{3g}$  and  $a_\gamma$ .

One may wonder why Gerard and Weyers's assertion seems to enjoy considerable success when applied to  $J/\psi$  decays, even though it looks theoretically ungrounded. One possible explanation is that, due to some specific dynamics, the relative strength and phase between electromagnetic and strong amplitudes are roughly identical for each  $J/\psi$  exclusive decay mode, preserving the same pattern as in the inclusive decay. This approximate scaling between exclusive and inclusive channels is exemplified in the discussion following (37). This pattern does not necessarily hold for other vector quarkonium decays.

It is straightforward to see that, the approximate  $-90^\circ$  phase between strong and electromagnetic amplitude in our process is simply a consequence of the not-too-tiny mass ratio  $m_c^2/m_b^2 \approx 0.1$  and the opposite electric charges of  $c$  and  $b$  (see left panel of Fig. 3 and (27)). It may seem to be a marvellous coincidence that the relative phase determined in our case is very close to that in  $J/\psi \rightarrow PV$ , especially regarding that the latter process should be largely dictated by nonperturbative long-distance dynamics. We don't know exactly which nonperturbative mechanism should be responsible for the universal orthogonal phase in various  $J/\psi$  decay modes. It is fun to notice that, however, in the constituent quark model, the masses of  $u$ ,  $d$  and  $s$  quarks are several hundreds of MeV, consequently  $m_{u,d,s}^2/m_c^2 \approx m_c^2/m_b^2$ , so our formalism seems to be able to explain the nearly orthogonal phase in  $J/\psi \rightarrow PV$  entirely within the short-distance quark-gluon picture.

Lastly we stress that the phases determined in (35) and (38) are subject to large uncertainties. Since they are determined only at the lowest-order accuracy, it is conceivable that they may receive large modifications by including radiative and relativistic corrections. Moreover, for simplicity we have assumed the radiative correction to electromagnetic amplitude does not introduce an imaginary part. One should realize this is just an (decent

---

<sup>2</sup> Besides the  $1^-0^-$  mode, other two-body decays of  $J/\psi$  seem to also have a nearly orthogonal relative phase between  $a_\gamma$  and  $a_{3g}$ , such as  $0^-0^-$  [15, 38],  $1^-1^-$  [1, 15, 38],  $1^+0^-$  [39] and  $N\bar{N}$  [15, 40]. Moreover in  $\psi'$  decays, the  $1^-0^-$  [41] and  $0^-0^-$  mode [42, 43] seem also compatible with a large relative phase.

TABLE III: The Breit-Wigner, continuum and full cross sections (in units of fb) for  $e^+e^- \rightarrow J/\psi + \eta_c$  at various  $\Upsilon(nS)$  resonances. All the input parameters are the same as in Section III B except  $\alpha_s$  is fixed to be 0.22.

$\sqrt{s}$ (GeV)	$\sigma_{\text{BW}}$	$\sigma_{\text{cont}}$	$\sigma_{\text{full}}$
9.460	15678	47.1	14158
10.023	7165	32.7	6317
10.355	7948	26.4	7141
10.579	0.0026	22.9	22.5

though) approximation. Despite this alertness, we still expect the qualitative feature, *i.e.*, the large relative phase can withstand all these uncertainties.

### C. Continuum-resonance interference for double charmonium production

For a given final state in  $e^+e^-$  annihilation experiment near a vector meson resonance, it is always produced via two inseparable mechanisms—resonant decay and continuum production. A rough indicator about the relative strength of resonant electromagnetic amplitude to the continuum amplitude is characterized by  $3\mathcal{B}_{e^+e^-}/\alpha$ . For the first four  $\Upsilon$  resonances, this factor is 10.2, 7.9, 8.9 and 0.0055 respectively. Therefore, for the three lower  $\Upsilon$  resonances, the  $J/\psi + \eta_c$  production are dominated by the resonant decay, whereas for the  $\Upsilon(4S)$ , which has a width about three orders of magnitude broader, one expects that the continuum contribution plays an overwhelmingly important role.

We are interested to know the impact of the resonance-continuum interference on the observed cross sections. Assuming  $a_\gamma$  and  $a_c$  differ by a Breit-Wigner propagator, one can express the full cross section near  $\Upsilon$  peak as

$$\sigma_{\text{full}}[e^+e^- \rightarrow J/\psi + \eta_c] = \sigma_{\mu^+\mu^-} \frac{2^{20} \pi^2 e_c^2 \alpha_s^2 |\mathbf{P}|^3}{9 s^{9/2}} \psi_{J/\psi}^2(0) \psi_{\eta_c}^2(0) \quad (39)$$

$$\times \left| K + \frac{3\alpha^{-1} \sqrt{s} \Gamma_{e^+e^-}}{s - M_\Upsilon^2 + i M_\Upsilon \Gamma_{\text{tot}}} (K + a_{3g} + a_{gg\gamma}) \right|^2,$$

where  $\Gamma_{e^+e^-}$  and  $\Gamma_{\text{tot}}$  are the electric and total width of  $\Upsilon$ . If the continuum term is dropped, this formula then reduces to the standard Breit-Wigner form:

$$\sigma_{\text{BW}}[e^+e^- \rightarrow \Upsilon \rightarrow J/\psi + \eta_c] = \frac{12\pi \Gamma_{e^+e^-} \Gamma[\Upsilon \rightarrow J/\psi + \eta_c]}{(s - M_\Upsilon^2)^2 + M_\Upsilon^2 \Gamma_{\text{tot}}^2}. \quad (40)$$

In Table III we have enumerated various contributions to the  $J/\psi + \eta_c$  cross sections at  $\Upsilon(nS)$  peaks. One can clearly see the inclusion of the continuum contribution will reduce the peak cross sections by about 10% for the first three  $\Upsilon$  states, whereas including the resonant contribution will reduce the continuum cross section by about 2% for  $\Upsilon(4S)$ . This destructive interference can be attributed to the approximate  $180^\circ$  relative phase between  $a_{3g}$  and  $a_c$ .



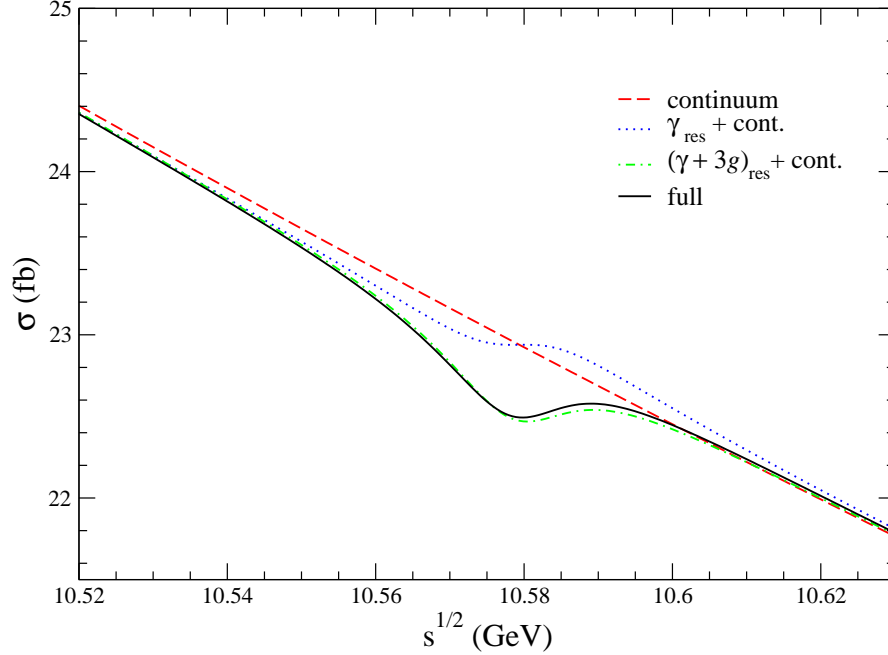


FIG. 5: The line shape of  $e^+e^- \rightarrow J/\psi + \eta_c$  near  $\sqrt{s} = M_{\Upsilon(4S)}$ .

The interference with continuum contribution also slightly distorts the Breit-Wigner shape of the production cross sections for the first three  $\Upsilon$  resonances. However, one has to bear in mind that, for a thorough analysis, one has to carefully take the beam spread and radiative corrections into account, which requires lots of extra work and we leave them to the experimentalists.

Thus far, the measured double charmonium production in  $B$  factories has been assumed to be entirely initiated by the continuum process, as represented in (32). Experimentally, the resonant decay, despite its small magnitude, is encapsulated in the observed cross sections. It is interesting to know how the line shape of  $J/\psi + \eta_c$  near  $\Upsilon(4S)$  peak would be affected by including this contribution. In Fig. 5, we have shown the various line shapes, with the contributions from several different sources juxtaposed. An interesting feature is that a dip is developed right on the  $\Upsilon(4S)$  peak, which is again due to the destructive interference between the resonant strong decay and continuum amplitudes. Furthermore, we are reassured again that the radiative decay amplitude is unimportant. It will be great if someday experimentalists can do an energy scan and pin down this dip structure. To achieve this goal, the cross section must be measured very precisely, of course a very challenging task. We finally remark that, due to the aforementioned destructive interference, the true continuum cross sections should be slightly larger than the values quoted in (34), which are in fact the full cross sections measured experimentally.

#### IV. SUMMARY AND OUTLOOK

In this work, we have performed a systematic study on  $\Upsilon$  exclusive decays to vector plus pseudoscalar charmonium in NRQCD factorization framework. These exclusive decay modes can proceed via three-gluon, one-photon and two-gluon-one-photon, each of which

has been thoroughly analyzed. The relative phases among these amplitudes naturally arise as a consequence of the short-distance loop contribution. A particularly interesting finding is that the relative phase between strong and electromagnetic amplitude is nearly orthogonal, which is the same as that in various  $J/\psi$  decay modes.

The typical branching fractions of these decays are predicted to be of order  $10^{-6}$  for the low-lying  $\Upsilon(nS)$  states ( $n = 1, 2, 3$ ). Future dedicated high-luminosity  $e^+e^-$  facilities, *e.g.* Super  $B$  experiment, should be able to discover these decay channels readily.

We have also investigated the impact of the continuum-resonance interference on the  $J/\psi + \eta_c$  production cross sections at different  $\Upsilon$  peaks. We find this interference will reduce the peak cross sections for the first three  $\Upsilon$  states by about 10%. We predict there is a small dip in the line shape on the  $\Upsilon(4S)$  peak. The current experiments are too rough to discern this delicate structure, perhaps the future Super  $B$  experiment can verify this prediction.

A natural extension of this work is to investigate other exclusive double charmonium production processes from  $\Upsilon$  decay. For example,  $\Upsilon \rightarrow \chi_{cJ} J/\psi$  are particularly interesting channels to study, since the inclusive bounds for  $\Upsilon \rightarrow \chi_{cJ} + X$  have already been experimentally available [8]. Besides these double charmonium decay modes, one may also be tempted to apply the same formalism developed in this work to the processes  $\Upsilon(J/\psi) \rightarrow PV$  [44]. For the scarcity of theoretical investigations to these decay modes from the angle of pQCD, this study will offer us something worthwhile learning. Although it will no longer be as theoretically well grounded as the processes considered in this work, it should be viewed as an approach rooted in the time-tested constituent quark model, which has witnessed many phenomenological successes over years.

## Acknowledgments

I am indebted to Chang-Zheng Yuan for comments on the manuscript. This work is supported in part by National Natural Science Foundation of China under Grant No. 10605031.

## APPENDIX A: DERIVING ANALYTICAL EXPRESSION FOR $f$

In this Appendix we illustrate how to simplify  $f$  effectively, so that we can obtain their analytical expressions. Repeatedly using kinematical relations stemming from the constraint  $k_1 + k_2 = \frac{Q}{2}$ , plus fractional decomposition, we can reduce each  $f_i$  in (11), (12) and (13) into

the sum of two-point tensor and three-point scalar integrals:

$$f_1(\xi) = \int \frac{d^4 k_1}{i\pi^2} \left\{ \frac{2m_b^2 - 3m_c^2}{k_1^2 k_2^2 (k_1^2 - k_1 \cdot P)} + \frac{k_1 \cdot (3Q - P)}{m_b^2} \left[ \frac{1}{k_1^2 k_2^2} - \frac{1}{k_1^2 (k_2^2 - m_b^2)} \right] \right. \\ \left. + \frac{k_1 \cdot [(2 - \xi)Q - P]}{m_b^2} \left[ \frac{1}{(k_2^2 - m_b^2)(k_1^2 - k_1 \cdot P)} - \frac{1}{k_2^2 (k_1^2 - k_1 \cdot P)} \right] \right\}, \quad (\text{A1})$$

$$f_2(\xi) = \int \frac{d^4 k_1}{i\pi^2} \left\{ \frac{m_b^2 - 3m_c^2}{k_1^2 k_2^2 (k_1^2 - k_1 \cdot P)} + \frac{k_2 \cdot P}{m_b^2} \left[ \frac{1}{k_1^2 k_2^2} - \frac{1}{(k_1^2 - m_b^2)k_2^2} \right] \right. \\ \left. + \frac{k_2 \cdot (P - \xi Q)}{m_b^2} \left[ \frac{1}{(k_1^2 - m_b^2)(k_1^2 - k_1 \cdot P)} - \frac{1}{k_1^2 (k_1^2 - k_1 \cdot P)} \right] \right\}, \quad (\text{A2})$$

$$f_3(\xi) = -2 \int \frac{d^4 k_1}{i\pi^2} \left\{ \frac{m_b^2 - 2m_c^2}{k_1^2 k_2^2 (k_1^2 - k_1 \cdot P)} + \frac{2m_c^2}{(k_1^2 - m_b^2)(k_2^2 - m_b^2)(k_1^2 - k_1 \cdot P)} \right. \\ \left. + \frac{1}{k_1^2 k_2^2} - \frac{1}{(k_1^2 - m_b^2)(k_2^2 - m_b^2)} + \frac{1}{(k_1^2 - m_b^2)(k_1^2 - k_1 \cdot P)} - \frac{1}{k_1^2 (k_1^2 - k_1 \cdot P)} \right\}, \quad (\text{A3})$$

where  $\xi = m_c^2/m_b^2$ . While the two-point functions can be trivially handled, working out the three-point scalar integrals is more laborious but still straightforward. Here we just give their analytic forms:

$$C_1(\xi) = \int \frac{d^4 k_1}{i\pi^2} \frac{m_b^2}{k_1^2 k_2^2 (k_1^2 - k_1 \cdot P)} \\ = -\frac{1}{\beta} \left\{ 2 \tanh^{-1} \beta \ln \xi + 2 \text{Li}_2 \left[ \frac{1 - \beta}{2} \right] - 2 \text{Li}_2 \left[ \frac{1 + \beta}{2} \right] \right. \\ \left. + \text{Li}_2 \left[ \frac{\beta - 1}{\beta + 1} \right] - \text{Li}_2 \left[ \frac{\beta + 1}{\beta - 1} \right] + 2\pi i \tanh^{-1} \beta \right\}. \quad (\text{A4})$$

$$C_2(\xi) = \int \frac{d^4 k_1}{i\pi^2} \frac{m_b^2}{(k_1^2 - m_b^2)(k_2^2 - m_b^2)(k_1^2 - k_1 \cdot P)} \\ = -\frac{1}{\beta} \left\{ \frac{2\pi}{3} \tan^{-1}[\sqrt{3}\beta] + 2 \tanh^{-1} \beta \ln[1 - 3\xi] + \text{Li}_2 \left[ \frac{2\beta}{1 + \beta} \right] - \text{Li}_2 \left[ \frac{2\beta}{\beta - 1} \right] \right. \\ + \text{Li}_2 \left[ \frac{\beta(\beta + 1)}{\beta - 1} \right] - \text{Li}_2 \left[ \frac{\beta(1 - \beta)}{1 + \beta} \right] + \text{Li}_2 \left[ \frac{\beta(1 + \beta)}{2(1 - 3\xi)} \right] - \text{Li}_2 \left[ \frac{\beta(\beta - 1)}{2(1 - 3\xi)} \right] \\ + \text{Li}_2 \left[ -\frac{\beta(1 - \beta)^2}{4(1 - 3\xi)} \right] - \text{Li}_2 \left[ \frac{\beta(1 + \beta)^2}{4(1 - 3\xi)} \right] \\ \left. + 2 \text{Re} \left\{ \text{Li}_2 \left[ -\frac{(1 + i\sqrt{3})\beta}{1 - i\sqrt{3}\beta} \right] - \text{Li}_2 \left[ \frac{(1 + i\sqrt{3})\beta}{1 + i\sqrt{3}\beta} \right] \right\} \right\}. \quad (\text{A5})$$

It may be worth mentioning that if the well-known master formula for massive three-point scalar integral (*i.e.*, equation (5.6) in [45]) is employed, one seems unable to obtain the correct expression for  $C_2$ . To be specific, using that formula would render  $C_2(\frac{1}{4}) = 0$ , which diametrically conflicts with the true value  $4 \ln 2 - 2\pi/\sqrt{3}$ . One can check our result is correct.

We now can express  $f_i$  as follows:

$$f_1(\xi) = (2 - 3\xi) C_1(\xi) + \frac{5}{2} + 2(3 - 2\xi) \left\{ \frac{1}{1 - \beta} \ln \left[ \frac{1 + \beta}{2} \right] + \frac{1}{1 + \beta} \ln \left[ \frac{1 - \beta}{2} \right] \right\} \\ - 2(1 + \xi) \left\{ \frac{1}{(1 - \beta)^2} \ln \left[ \frac{1 + \beta}{2} \right] + \frac{1}{(1 + \beta)^2} \ln \left[ \frac{1 - \beta}{2} \right] + \frac{1}{4\xi} \right\} + \frac{5i\pi}{2}, \quad (\text{A6})$$

$$f_2(\xi) = (1 - 3\xi) C_1(\xi) + \frac{1}{2} + 2(1 - 2\xi) \left\{ \frac{1}{1 - \beta} \ln \left[ \frac{1 + \beta}{2} \right] + \frac{1}{1 + \beta} \ln \left[ \frac{1 - \beta}{2} \right] \right\} \\ - 2\xi \left\{ \frac{1}{(1 - \beta)^2} \ln \left[ \frac{1 + \beta}{2} \right] + \frac{1}{(1 + \beta)^2} \ln \left[ \frac{1 - \beta}{2} \right] + \frac{1}{4\xi} \right\} + \frac{i\pi}{2}, \quad (\text{A7})$$

$$f_3(\xi) = -2(1 - 2\xi) C_1(\xi) - 4\xi C_2(\xi) - 4 \left\{ \frac{1}{1 - \beta} \ln \left[ \frac{1 + \beta}{2} \right] + \frac{1}{1 + \beta} \ln \left[ \frac{1 - \beta}{2} \right] \right\} \\ - \frac{2\pi}{\sqrt{3}} - 2i\pi. \quad (\text{A8})$$

Adding these three functions together then reproduces (14) and (15).

## APPENDIX B: DERIVING ANALYTICAL EXPRESSION FOR $g$

In this Appendix we illustrate how to reduce the one-loop four-point function in (20) to the sum of simpler two- and three-point scalar integrals. With the aid of the kinematical identities arising from the constraint  $k_1 + k_2 = \tilde{P}$ , we can disentangle this integral into three pieces:

$$g(\xi) = g_1(\xi) + g_2(\xi) + g_3(\xi), \quad (\text{B1})$$

where  $\xi = m_c^2/m_b^2$ , and

$$g_1(\xi) = \frac{1}{2} \int \frac{d^4 k_1}{i\pi^2} \frac{1}{k_1^2} \left[ \frac{1}{k_1^2 - k_1 \cdot Q} - \frac{1}{k_2^2 - k_2 \cdot Q} \right], \quad (\text{B2})$$

$$g_2(\xi) = \frac{2m_c^2}{m_b^2} \int \frac{d^4 k_1}{i\pi^2} \left[ \frac{1}{k_1^2} - \frac{1}{k_1^2 - k_1 \cdot Q} \right] \frac{1}{k_2^2 - k_2 \cdot Q} \\ + 2 \int \frac{d^4 k_1}{i\pi^2} \frac{m_c^2}{k_1^2 (k_1^2 - k_1 \cdot Q) (k_2^2 - k_2 \cdot Q)}, \quad (\text{B3})$$

$$g_3(\xi) = \frac{2(m_b^2 - 4m_c^2)}{m_b^2} \int \frac{d^4 k_1}{i\pi^2} \left[ \frac{m_c^2}{k_1^2 k_2^2 (k_1^2 - k_1 \cdot Q)} + \frac{m_b^2 - m_c^2}{k_1^2 (k_1^2 - k_1 \cdot Q) (k_2^2 - k_2 \cdot Q)} \right]. \quad (\text{B4})$$

Here we give the analytical expressions of two needed scalar 3-point integrals:

$$\begin{aligned}\tilde{C}_1(\xi) &= \int \frac{d^4 k_1}{i\pi^2} \frac{m_b^2}{k_1^2 k_2^2 (k_1^2 - k_1 \cdot Q)} \\ &= -\frac{1}{2\beta} \left\{ 4 \tanh^{-1} \beta \ln[2\xi] + 2 \text{Li}_2[-\beta] - 2 \text{Li}_2[\beta] + \text{Li}_2 \left[ \frac{\beta-1}{\beta+1} \right] \right. \\ &\quad \left. - \text{Li}_2 \left[ \frac{1+\beta}{\beta-1} \right] + \text{Li}_2 \left[ \frac{2\beta}{(1+\beta)^2} \right] - \text{Li}_2 \left[ -\frac{2\beta}{(1-\beta)^2} \right] + 2\pi i \tanh^{-1} \beta \right\},\end{aligned}\quad (\text{B5})$$

$$\begin{aligned}\tilde{C}_2(\xi) &= \int \frac{d^4 k_1}{i\pi^2} \frac{m_b^2}{k_1^2 (k_1^2 - k_1 \cdot Q) (k_2^2 - k_2 \cdot Q)} \\ &= -\frac{1}{2\beta} \left\{ \text{Li}_2[\beta] - \text{Li}_2[-\beta] + 2 \text{Re} \left\{ \text{Li}_2 \left[ \frac{(1+\beta)^2 + 4i\sqrt{\xi(1-\xi)}}{4(1-2\xi)} \right] \right. \right. \\ &\quad \left. - \text{Li}_2 \left[ \frac{(1-\beta)^2 + 4i\sqrt{\xi(1-\xi)}}{4(1-2\xi)} \right] + \text{Li}_2 \left[ -\frac{\beta(1-\beta)^2 + 4i\beta\sqrt{\xi(1-\xi)}}{4(1-2\xi)} \right] \right. \\ &\quad \left. \left. - \text{Li}_2 \left[ \frac{\beta(1+\beta)^2 + 4i\beta\sqrt{\xi(1-\xi)}}{4(1-2\xi)} \right] \right\} \right\}.\end{aligned}\quad (\text{B6})$$

Therefore we have

$$g_1(\xi) = \frac{1-2\xi}{1-4\xi} \ln[2-4\xi], \quad (\text{B7})$$

$$g_2(u) = 4\xi \left( \sqrt{\frac{1-\xi}{\xi}} \tan^{-1} \sqrt{\frac{\xi}{1-\xi}} - \frac{1-2\xi}{1-4\xi} \ln[2-4\xi] \right) + 2\xi \tilde{C}_2(u), \quad (\text{B8})$$

$$g_3(\xi) = 2(1-4\xi)[\xi \tilde{C}_1(\xi) + (1-\xi) \tilde{C}_2(\xi)]. \quad (\text{B9})$$

One then readily reproduces the analytic results shown in (21) and (22).

- 
- [1] L. Kopke and N. Wermes, Phys. Rept. **174**, 67 (1989).
  - [2] N. Brambilla *et al*, CERN-2005-005 [arXiv:hep-ph/0412158].
  - [3] G. T. Bodwin, E. Braaten and G. P. Lepage, Phys. Rev. D **51**, 1125 (1995) [Erratum-ibid. D **55**, 5853 (1997)] [arXiv:hep-ph/9407339].
  - [4] V. V. Braguta, A. K. Likhoded and A. V. Luchinsky, Phys. Rev. D **72**, 094018 (2005) [arXiv:hep-ph/0506009].
  - [5] Y. Jia, arXiv:hep-ph/0611130.
  - [6] W. S. Maschmann *et al*. [Crystal Ball Collaboration], Z. Phys. C **46**, 555 (1990).
  - [7] K. Abe *et al*. [BELLE Collaboration], Phys. Rev. Lett. **88**, 052001 (2002) [arXiv:hep-ex/0110012].
  - [8] R. A. Briere *et al*. [CLEO Collaboration], Phys. Rev. D **70**, 072001 (2004) [arXiv:hep-ex/0407030].
  - [9] S. J. Brodsky and G. P. Lepage, Phys. Rev. D **24**, 2848 (1981).
  - [10] V. L. Chernyak and A. R. Zhitnitsky, Phys. Rept. **112**, 173 (1984);

- [11] K. Abe *et al.* [Belle Collaboration], Phys. Rev. Lett. **89**, 142001 (2002) [arXiv:hep-ex/0205104].
- [12] R. M. Baltrusaitis *et al.* [MARK-III Collaboration], Phys. Rev. D **32**, 2883 (1985).
- [13] D. Coffman *et al.* [MARK-III Collaboration], Phys. Rev. D **38**, 2695 (1988) [Erratum-ibid. D **40**, 3788 (1989)].
- [14] J. Jousset *et al.* [DM2 Collaboration], Phys. Rev. D **41**, 1389 (1990).
- [15] G. Lopez Castro, J. L. Lucio M. and J. Pestieau, AIP Conf. Proc. **342**, 441 (1995) [arXiv:hep-ph/9902300].
- [16] M. Suzuki, Phys. Rev. D **57**, 5717 (1998) [arXiv:hep-ph/9801284].
- [17] N. N. Achasov, AIP Conf. Proc. **619**, 649 (2002) [arXiv:hep-ph/0110057].
- [18] For a recent review on the status of  $\rho\pi$  puzzle, see X. H. Mo, C. Z. Yuan and P. Wang, arXiv:hep-ph/0611214.
- [19] T. Li, S. M. Zhao and X. Q. Li, arXiv:0705.1195 [hep-ph].
- [20] B. Guberina and J. H. Kuhn, Lett. Nuovo Cim. **32**, 295 (1981).
- [21] E. Braaten and J. Lee, Phys. Rev. D **67**, 054007 (2003) [Erratum-ibid. D **72**, 099901 (2005)] [arXiv:hep-ph/0211085].
- [22] K. Y. Liu, Z. G. He and K. T. Chao, Phys. Lett. B **557**, 45 (2003) [arXiv:hep-ph/0211181].
- [23] G. T. Bodwin, J. Lee and E. Braaten, Phys. Rev. Lett. **90**, 162001 (2003) [arXiv:hep-ph/0212181].
- [24] G. T. Bodwin, J. Lee and E. Braaten, Phys. Rev. D **67**, 054023 (2003) [Erratum-ibid. D **72**, 099904 (2005)] [arXiv:hep-ph/0212352].
- [25] K. Hagiwara, E. Kou and C. F. Qiao, Phys. Lett. B **570**, 39 (2003) [arXiv:hep-ph/0305102].
- [26] J. P. Ma and Z. G. Si, Phys. Rev. D **70**, 074007 (2004) [arXiv:hep-ph/0405111].
- [27] A. E. Bondar and V. L. Chernyak, Phys. Lett. B **612**, 215 (2005) [arXiv:hep-ph/0412335].
- [28] Y. J. Zhang, Y. j. Gao and K. T. Chao, Phys. Rev. Lett. **96**, 092001 (2006) [arXiv:hep-ph/0506076].
- [29] G. T. Bodwin, D. Kang and J. Lee, Phys. Rev. D **74**, 114028 (2006) [arXiv:hep-ph/0603185].
- [30] Z. G. He, Y. Fan and K. T. Chao, Phys. Rev. D **75**, 074011 (2007) [arXiv:hep-ph/0702239].
- [31] W. M. Yao *et al.* [Particle Data Group], J. Phys. G **33**, 1 (2006).
- [32] K. Abe *et al.* [Belle Collaboration], Phys. Rev. D **70**, 071102 (2004) [arXiv:hep-ex/0407009].
- [33] B. Aubert *et al.* [BABAR Collaboration], Phys. Rev. D **72**, 031101 (2005) [arXiv:hep-ex/0506062].
- [34] R. Ammar *et al.* [CLEO Collaboration], Phys. Rev. D **57**, 1350 (1998) [arXiv:hep-ex/9707018].
- [35] S. Eidelman *et al.* [Particle Data Group], Phys. Lett. B **592**, 1 (2004).
- [36] D. Besson *et al.* [CLEO Collaboration], Phys. Rev. D **74**, 012003 (2006) [arXiv:hep-ex/0512061].
- [37] J. M. Gerard and J. Weyers, Phys. Lett. B **462**, 324 (1999) [arXiv:hep-ph/9906357].
- [38] M. Suzuki, Phys. Rev. D **60**, 051501 (1999) [arXiv:hep-ph/9901327].
- [39] M. Suzuki, Phys. Rev. D **63**, 054021 (2001).
- [40] R. Baldini *et al.*, Phys. Lett. B **444**, 111 (1998).
- [41] P. Wang, C. Z. Yuan and X. H. Mo, Phys. Rev. D **69**, 057502 (2004) [arXiv:hep-ph/0303144].
- [42] C. Z. Yuan, P. Wang and X. H. Mo, Phys. Lett. B **567**, 73 (2003) [arXiv:hep-ph/0305259].
- [43] S. Dobbs *et al.* [CLEO Collaboration], Phys. Rev. D **74**, 011105 (2006) [arXiv:hep-ex/0603020].
- [44] Y. Jia, in preparation.
- [45] G. 't Hooft and M. J. G. Veltman, Nucl. Phys. B **153**, 365 (1979).